LETTERS

Simulated Tropical Response to a Substantial Weakening of the Atlantic Thermohaline Circulation

RONG ZHANG

GFDL/AOS Program, Princeton University, Princeton, New Jersey

THOMAS L. DELWORTH

NOAA/GFDL, Princeton, New Jersey

(Manuscript received 4 January 2005, in final form 25 February 2005)

ABSTRACT

In this study, a mechanism is demonstrated whereby a large reduction in the Atlantic thermohaline circulation (THC) can induce global-scale changes in the Tropics that are consistent with paleoevidence of the global synchronization of millennial-scale abrupt climate change. Using GFDL's newly developed global coupled ocean–atmosphere model (CM2.0), the global response to a sustained addition of freshwater to the model's North Atlantic is simulated. This freshwater forcing substantially weakens the Atlantic THC, resulting in a southward shift of the intertropical convergence zone over the Atlantic and Pacific, an El Niño–like pattern in the southeastern tropical Pacific, and weakened Indian and Asian summer monsoons through air–sea interactions.

1. Introduction

Paleorecords show that Late Pleistocene climate changes at many different regions were coherent with the millennial-scale Dansgaard–Oeschger (D–O) cycles recorded in the Greenland ice core. For example, when Greenland was in stadial (cooling) condition, the summer Asian monsoon was reduced as indicated by a record from Hulu Cave in eastern China (Wang et al. 2001), and the Indian summer monsoon was weakened (Altabet et al. 2002). Stott et al. (2002) suggests that Greenland stadials were related to an El Niño–like pattern of sea surface temperature (SST) change, a weakened Walker circulation, and a southward shift of the intertropical convergence zone (ITCZ) in the tropical Pacific. An El Niño–like pattern occurred during the Last Glacial Maximum with reduced cross-equatorial and east–west SST contrasts in the tropical Pacific, and the tropical Pacific east–west SST contrast was further reduced during the Heinrich (H1) and Younger Dryas events (Lea et al. 2000; Koutavas et al. 2002). Wet periods in northeastern Brazil are synchronous with Heinrich events, cold periods in Greenland, and periods of weak east Asian summer monsoons and decreased river runoff to the Cariaco Basin (Wang et al. 2004). Those remote signals were extremely strong during H1 when the thermohaline circulation (THC) was almost shutdown (McManus et al. 2004). It is not clear whether abrupt climate change over Greenland is triggered by tropical variability (Clement et al. 2001; Latif 2001), or vice versa (Clark et al. 2002).

Previous coupled modeling studies (Vellinga and Wood 2002; Dahl et al. 2005, hereafter DBS) have shown a weakened THC, cooling in the North Atlantic, and warming in the South Atlantic in response to freshwater forcing in the North Atlantic, while very few responses were found in the Tropics outside the Atlantic. With a very strong transient freshwater forcing inserted in the North Atlantic at the initial stage of the experiment, Dong and Sutton (2002) showed that a sudden weakening of the THC leads to an El Niño event at year 7 of the simulation. In the present study, using a coupled ocean–atmosphere model, we show that a

Corresponding author address: Rong Zhang, GFDL/AOS Program, Princeton University, Princeton, NJ 08542.
E-mail: Rong.Zhang@noaa.gov

steady freshwater forcing in the North Atlantic leads to persistent remote responses in the tropical Pacific and a weakening of the Indian and Asian summer monsoons, consistent with the global synchronization of abrupt climate change indicated by paleorecords.

2. Description of experiments and local responses in the Atlantic

The model we employed here is the fully coupled ocean–atmosphere global general circulation model (CM2.0) developed at the Geophysical Fluid Dynamics Laboratory (GFDL). The ocean model employs an explicit free surface and a true freshwater flux exchange between the ocean and atmosphere. It has 50 vertical levels (22 levels of 10-m thickness each in the top 220 m), and 1° zonal resolution. The meridional resolution is 1° outside the Tropics and refined to 1/3° at the equator. The atmosphere model has 24 vertical levels, with horizontal resolution of 2° latitude × 2.5° longitude. The model uses 1860 radiative forcing conditions, including the solar irradiance, and produces a stable realistic multicentury control integration without flux adjustments (Delworth et al. 2005, manuscript submitted to *J. Climate*, hereafter D05).

To explore the response of the global climate to a weakening of the Atlantic thermohaline circulation, a perturbation experiment is conducted in which an extra freshwater forcing of 0.6 Sv (1 Sv $\equiv 10^6$ m^3 s^{-1}) is uniformly distributed over the northern North Atlantic (55°–75°N, 63°W–4°E) for the entire 60-yr duration of the experiment. The amplitude of the forcing is relatively large in order to elicit a clear response. In the perturbed experiment, the maximum Atlantic THC rapidly weakens from 16 Sv (time mean in the control run) to about 6 Sv after 20 yr, after which the rate of decrease gradually slows, resulting in an average of 4 Sv from years 21 to 60 (Fig. 1a). (The analyses shown below are focused on the differences between the two experiments averaged over years 21 to 60; all quantities shown are annual mean, unless indicated otherwise.) This substantial weakening of the THC weakens the global ocean northward cross-equatorial heat transport by 0.28 PW and strengthens the global atmospheric northward cross-equatorial heat transport by 0.32 PW (Fig. 1b). It also induces the typical dipole SST anomaly: cooling in the North Atlantic and warming at the equator and the South Atlantic (Fig. 1c) and a southward shift of the ITCZ over the tropical Atlantic (Fig. 1d), similar to previous simulations (Vellinga and Wood 2002; DBS) and consistent with the interpretation of paleoproxies of drying over the Cariaco Basin (Peterson et al. 2000) and wetting over northeastern Brazil (Wang et al. 2004) during Greenland cooling. The southward ITCZ shift is associated with an anomalous Hadley cell over the Atlantic, with a descending branch at 10°N and a near-surface ascending branch at the equator (Fig. 1g).

3. Remote responses in the tropical Pacific and the mechanism

The Atlantic changes induce many significant responses in the Pacific, including a warming (0.4 K) over the eastern tropical Pacific cold tongue south of the equator (Fig. 1c), an enhancement of precipitation in the southern central tropical Pacific by 1 m yr^{-1}, and a reduction of precipitation in the southern western Pacific warm pool (WPWP) by 0.8 m yr^{-1} (Fig. 1d), indicating a weakened and eastward shift of the Walker circulation there. North of the equator, there is cooling (1 K) in the eastern tropical Pacific off the coast of central America (Fig. 1c), a reduction of precipitation in the northern-central tropical Pacific by 0.8 m yr^{-1}, consistent with the paleorecord of drying and cooling condition during the H1 over the eastern Pacific north of the equator (Benway et al. 2004). There is also an enhancement of precipitation in the northern WPWP by 0.5 m yr^{-1} (Fig. 1d), indicating a strengthened Walker circulation there. The eastern tropical Pacific anomaly triggered by the substantially weakened THC is opposite across the equator, with an El Niño–like pattern to the south and a La Niña–like pattern to the north. The terms "El Niño–like" and "La Niña–like" are used for analogy to the spatial pattern of El Niño or La Niña. The responses we show are changes in the mean state, not transient oscillations. The ITCZ in the central Pacific weakens to the north of the equator and strengthens to the south of the equator, that is, it becomes more symmetric about the equator. The anomalous Hadley cell over the eastern Pacific has an ascending branch around 10°S and a descending branch around 10°N (Fig. 1h).

The global zonally averaged precipitation minus evaporation (P − E) is enhanced by 0.23 m yr^{-1} around 10°S, and reduced by 0.39 m yr^{-1} around 10°N (Fig. 1e), indicating an anomalous southward moisture transport across the equator. The global zonally integrated anomalous Hadley cell has a maximum of 32×10^9 kg s^{-1} (Fig. 1f), consistent with the enhanced atmospheric northward heat transport and the zonally averaged P − E anomaly (Figs. 1b,e). The positive peak of the P − E anomaly around 10°S and the ascending branch of the anomalous Hadley cell there (Figs. 1e,f) are mainly caused by the enhancement of the tropical Pacific ITCZ south of the equator (Fig. 1h). The mod-

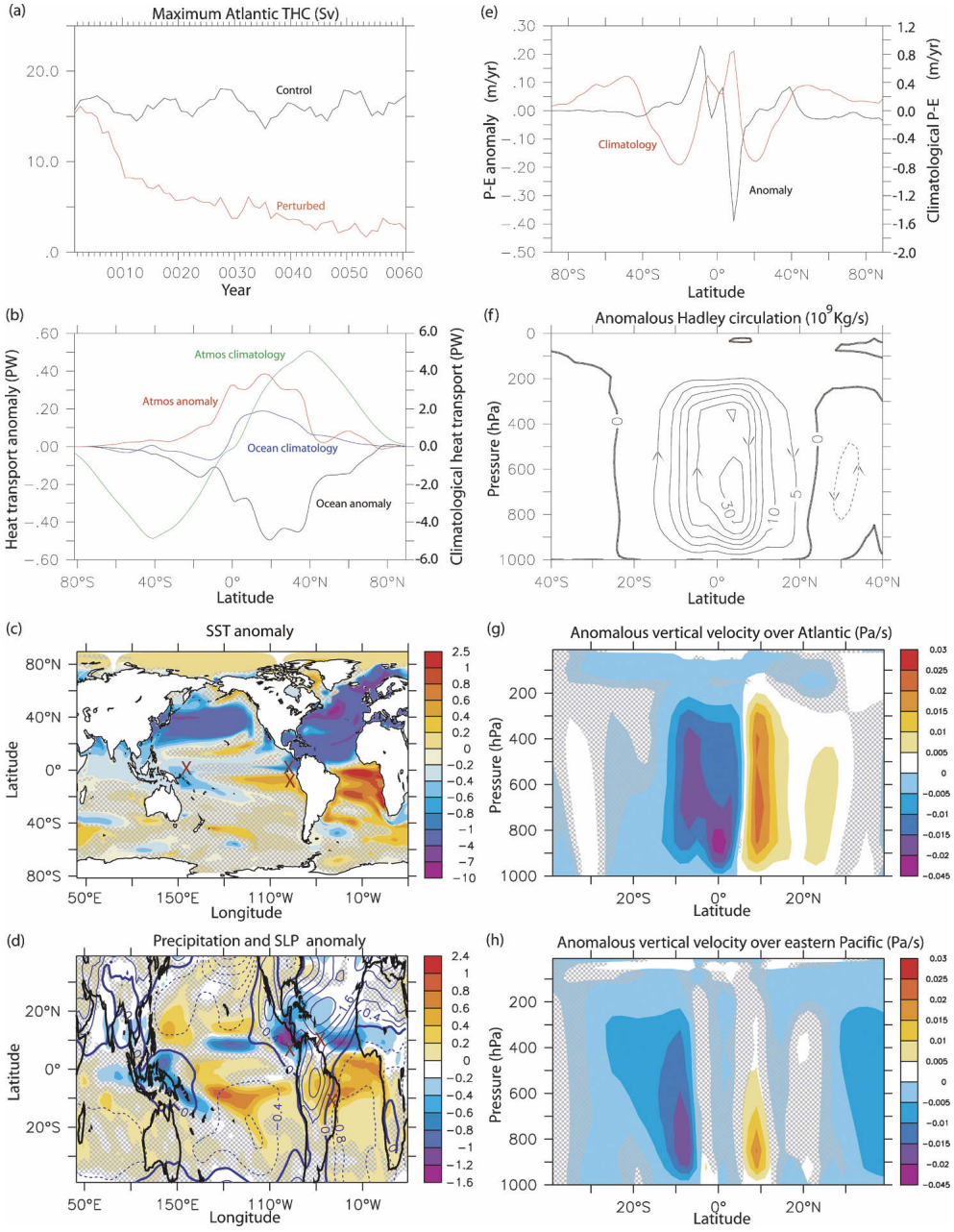

FIG. 1. Results from the coupled model using the OGCM: (a) Time series of the max Atlantic THC (max value of the annual Eulerian mean overturning streamfunction over the domain 30°–80°N in the North Atlantic) in the control and perturbed experiments, respectively. (b) Annual mean atmospheric and ocean heat transport anomaly (PW), along with the climatological atmospheric and ocean heat transport (PW) (averaged from years 21 to 60 of the control experiment). The "anomaly" is defined as the 40-yr (from years 21 to 60) averaged difference (perturbed − control). (c) Annual mean SST anomaly (K). Brown crosses mark the location of paleoproxies of SST in the tropical Pacific (Lea et al. 2000; Koutavas et al. 2002). (d) Annual mean precipitation anomaly (m yr^{-1}). The blue contour is the annual mean SLP anomaly with an interval of 0.4 hPa. The brown crosses mark the location of paleoproxies of precipitation at the Cariaco Basin (Peterson et al. 2000), northeastern Brazil (Wang et al. 2004), and the northeastern tropical Pacific (Benway et al. 2004). (e) Annual mean zonal averaged P − E anomaly (m yr^{-1}), along with the climatological value (m yr^{-1}). (f) Annual mean zonal integrated atmosphere streamfunction anomaly (10^9 kg s^{-1}). (g) Anomalous pressure vertical velocity (ω; Pa s^{-1}) averaged over the Atlantic (50°W–0°); negative values indicate upward motion. (h) Same as in (g), but averaged over the eastern Pacific (150°–100°W). The anomalies are significant at the 95% level in area without shadow and are not significant at the 95% level in area with shadow with Student's t test.

eled global zonally integrated Hadley circulation and zonally averaged ITCZ become more symmetric about the equator when the THC is substantially weakened.

The detailed link of the response from the Atlantic to the tropical Pacific is through the central American region, where precipitation is reduced by 1.2 m yr^{-1} because of strong cooling in the tropical Atlantic off the central American coast. This cooling enhances sea level pressure (SLP) in the eastern tropical Pacific off the Central American coast (Fig. 1d), which weakens the climatological Hadley circulation in the eastern tropical Pacific and induces anomalous southward surface winds across the equator in the eastern Pacific. This southward surface wind anomaly induces anomalous ocean upwelling and thus cooling in the eastern tropical Pacific north of the equator, and anomalous ocean downwelling and thus warming in the cold tongue south of the equator. A negative SLP anomaly develops over the southeastern Pacific cold tongue (Fig. 1d). The SST dipole anomaly across the eastern tropical Pacific further amplifies the anomalous southward wind flow, moisture transport, ITCZ shift, and the anomalous Hadley circulation (Fig. 1h). Hence the southeast trade wind and thus the Walker circulation south of the equator are weakened, and the upwelling in the southeastern Pacific is further weakened. The northeast trade wind and thus the Walker circulation north of the equator are enhanced, and the upwelling in the northeastern Pacific is further enhanced. The vertical velocity anomaly at 500 mb (Fig. 2a) has a very similar pattern as the precipitation anomaly, indicating the changes in the background Walker circulations. The eastward shift of the Walker circulation extends from about 15°S to the equator with a northwest tilt (Fig. 2a). The westward zonal surface wind stress anomaly reaches a maximum of 0.018 N m^{-2} over the northeastern tropical Pacific, and the eastward zonal surface wind stress anomaly is 0.01 N m^{-2} over the southern-central tropical Pacific. The southward meridional surface wind stress anomaly is 0.01 N m^{-2} over the central and eastern tropical Pacific.

South of the equator, the western tropical Pacific thermocline is shallowed because of the weakened southeast trade wind, resulting in surface and subsurface cooling there (Fig. 2b), similar to that in an El Niño phase. This reduces the east–west SST contrast at 10°S and provides a positive feedback to the weakening and eastward shift of the Walker circulation there. North of the equator, the western tropical Pacific thermocline is deepened as a result of the enhanced northeast trade wind, resulting in subsurface warming there (Fig. 2c), similar to that in a La Niña phase. The thermocline depth variations, which cause the dipole subsurface temperature anomaly in Fig. 2c, correspond to a maximum decrease (increase) of sea surface height (SSH) at 10°S (10°N), as they are both driven by surface wind anomalies. With the geostrophic balance, this weakens the northern equatorial counter current (NECC; 0.2 m s^{-1} in the control run; 0.14 m s^{-1} in the perturbed run) and strengthens the southern equatorial counter current (SECC; almost zero in the control run; 0.1m s^{-1} in the perturbed run; Fig. 2d). In modern climate, the NECC is much stronger and the SECC almost disappears because of the asymmetry of the Pacific ITCZ position. In the perturbed run, the western tropical Pacific Ocean circulation becomes more symmetric about the equator, along with the southward shift of the Pacific ITCZ. The mechanism of the tropical response discussed above is summarized in Fig. 2e.

The total clouds are reduced over the northeastern tropical Pacific, and their dominant effect is increasing downward shortwave surface heat flux there. Similarly, the total clouds are enhanced over the southern central tropical Pacific, and their dominant effect is decreasing downward shortwave surface heat flux there. These changes provide a negative feedback to the SST anomaly. Most of the SST anomaly in the tropical Pacific is in phase with the convergence of the oceanic heat transport anomaly, and the net atmospheric downward surface heat flux provides a negative feedback to the SST anomaly induced by the ocean dynamics.

Both cross-equatorial SST contrast in the eastern tropical Pacific and east–west SST contrast in the southern tropical Pacific are reduced by 1 K (Fig. 1c) as a result of the weakening of the THC, consistent with interpretations of paleorecords that reductions of the tropical Pacific cross-equatorial and east–west SST contrast are correlated with the Greenland cooling (Koutavas et al. 2002). It is difficult to compare directly with Pacific paleoproxies near the equator, as the maximum simulated response is off the equator with opposite phases on either side. We repeated this water hosing experiment with another newly developed GFDL fully coupled model (CM2.1; D05) that has a different atmospheric dynamic core and initial condition. The Pacific responses are very similar and robust, because both models have the same resolutions in the atmosphere and ocean components and are able to simulate the same physical mechanism causing such responses. The strong cooling over the North Atlantic excites a large-scale stationary wave pattern, resulting in an anomalous cyclonic surface wind and thus strong cooling over the extratropical north Pacific (Fig. 1c), similar to that in Vellinga and Wood (2002). This is opposite to the simulated warming over the extratropical North Pacific in response to a weakening of the THC (Saenko et al.

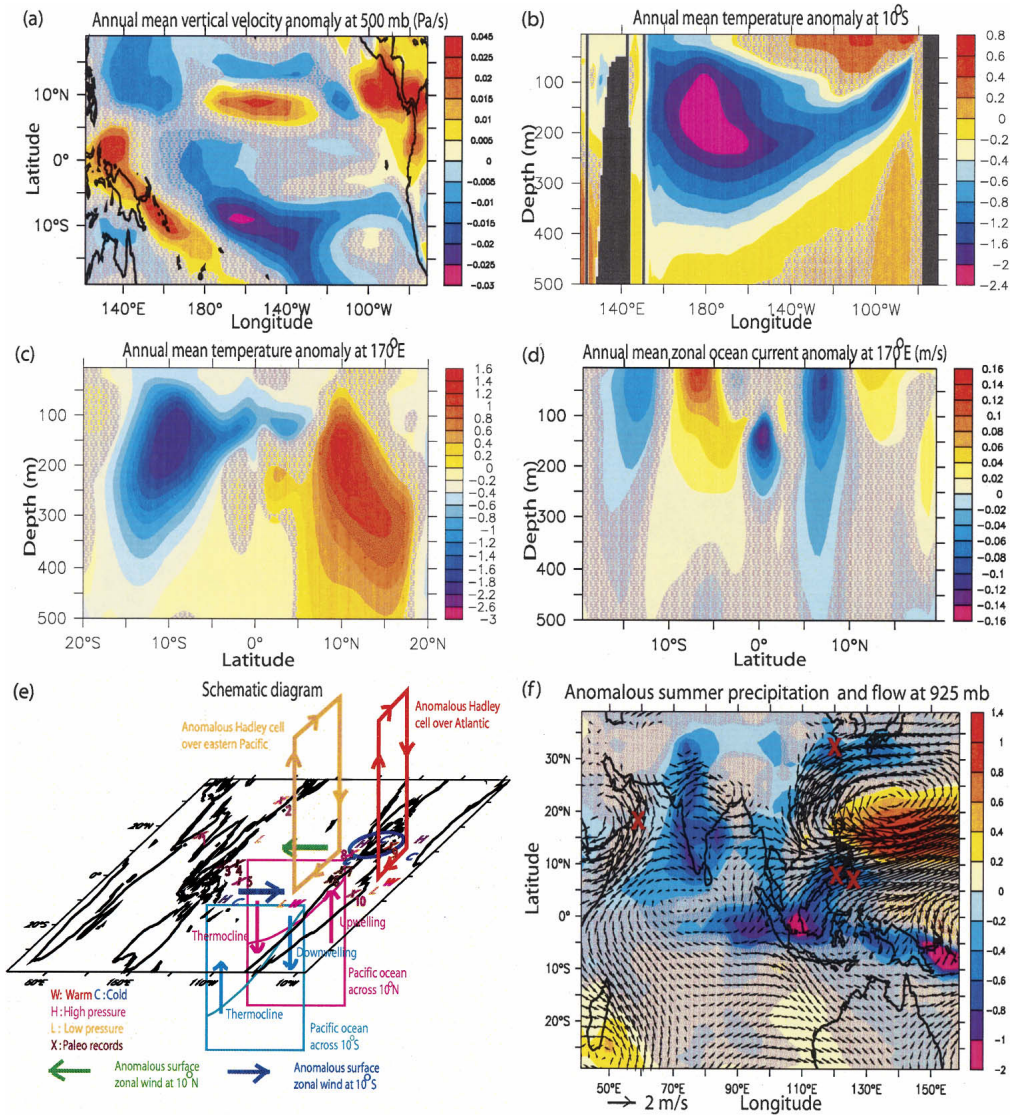

FIG. 2. Results from the coupled model using the OGCM and the schematic mechanism: (a) Annual mean pressure vertical velocity anomaly (ω; Pa s^{-1}) at 500 mb over the tropical Pacific; negative values indicate upward motion. (b) Annual mean ocean temperature anomaly (K) across 10°S in the tropical Pacific. (c) Same as in (b), but across 170°E in the tropical Pacific. (d) Annual mean zonal ocean current anomaly (m s^{-1}) across 170°E in the tropical Pacific. (e) Schematic diagram of global tropical responses to the North Atlantic freshwater forcing and the mechanism. The blue circle over the Central American coast emphasizes the important region of atmospheric linkage between the Atlantic and Pacific. The anomalous surface zonal wind over the northern tropical Pacific strengthens the trade wind there, while over the southern tropical Pacific, it weakens the trade wind. Brown crosses mark locations of paleoproxies: 1) Altabet et al. (2002), 2) Wang et al. (2001), 3) Dannenmann et al. (2003), 4) Stott et al. (2002), 5) Lea et al. (2000), 6) Koutavas et al. (2002), 7) Lea et al. (2000), 8) Benway et al. (2004), 9) Peterson et al. (2000), and 10) Wang et al. (2004). (f) Anomalous summer precipitation (m yr^{-1}) and flow at 925 hPa over the Indian and eastern China regions. Brown crosses mark paleoproxies at location 1, 2, 3, and 4 in (e). The SST and precipitation anomalies are significant at the 95% level in area without shadow and are not significant at the 95% level in area with shadow with Student's t test.

2004), and further investigations are necessary to reconcile the different model results.

To test the mechanism of the tropical response discussed above, we replaced the ocean general circulation model (OGCM) in the coupled model with a motionless slab ocean model with a single layer of depth of 50 m, interacting with the atmosphere through air–sea heat fluxes. A global climatological heat flux ("q flux"),

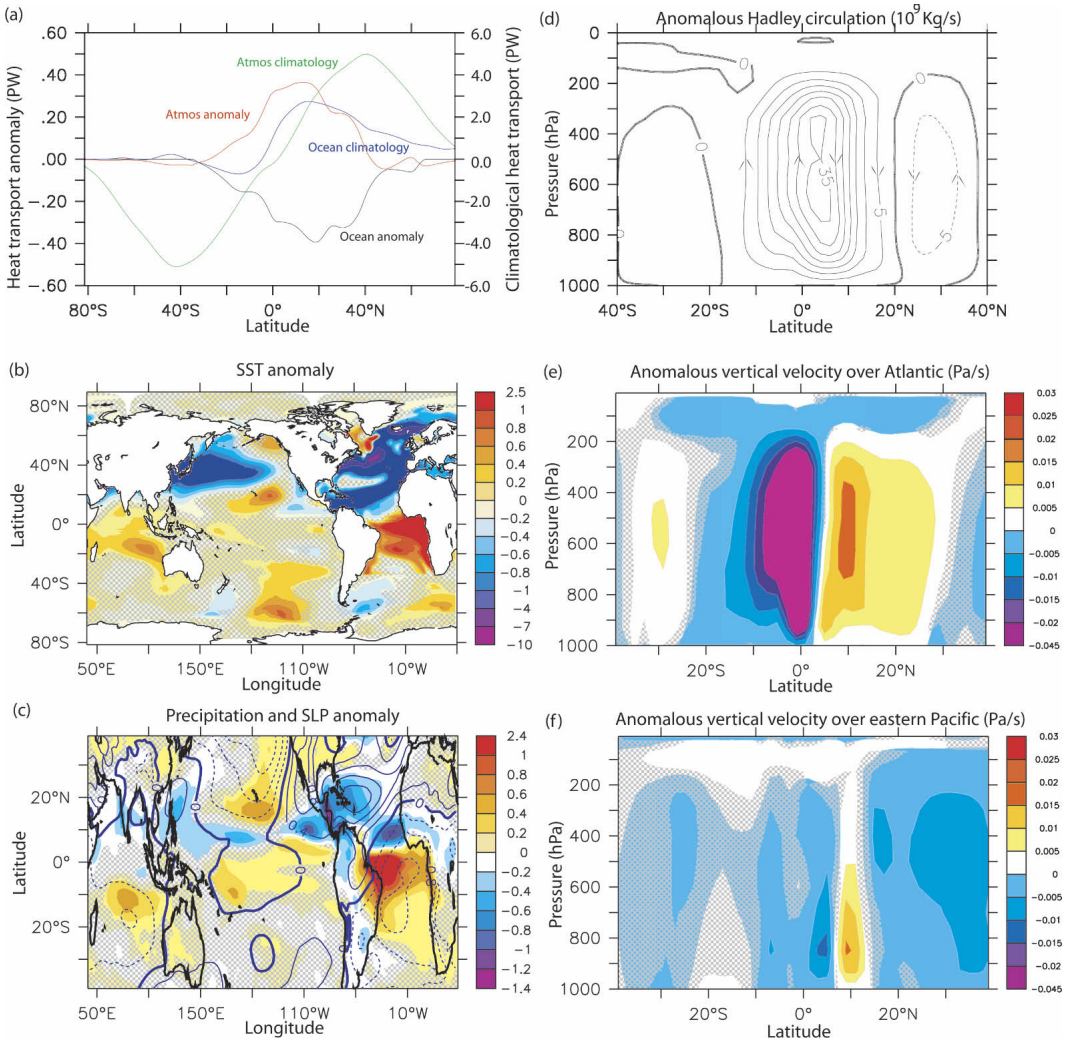

FIG. 3. Results from the coupled model using the slab ocean model: (a) Annual mean atmospheric and ocean heat transport anomaly (PW), along with the climatological atmospheric and ocean heat transport (PW; averaged from years 1 to 40 in the control experiment). The ocean heat transport is implied from the applied q flux. The Atlantic surface heat flux anomaly is similar to that in the fully coupled model because it is in balance with the applied q-flux anomaly. (b) Annual mean SST anomaly (K). (c) Annual mean precipitation anomaly (m yr^{-1}). The blue contour is the annual mean SLP anomaly with an interval of 0.4 hPa. (d) Annual mean zonal integrated atmosphere streamfunction anomaly (10^9 kg s^{-1}). (e), (f) Same as in Figs. 1g,h, respectively.

representing the effect of horizontal heat transport convergence in the ocean and heat exchange between the mixed layer and deep ocean, is prescribed with a repeating seasonal cycle. This helps to maintain climatological SST close to observations. In the perturbed run, an anomalous q flux (based on the negative of the Atlantic surface heat flux anomaly taken from the fully coupled model) is added only in the Atlantic for a 40-yr duration and gives the same implied cross-equatorial ocean northward heat transport reduction (0.28 PW; Fig. 3a) as the fully coupled model. The responses of many fields (computed as the 40-yr-averaged differences between the perturbed and control runs) are similar to those in the fully coupled model (cf. Figs. 1 and 3). These include cooling in the North Atlantic and warming in the South Atlantic, an anomalous Hadley cell and a southward shift of the ITCZ over the Atlantic, and an anomalous global integrated Hadley cell (38 $\times$ 10^9 kg s^{-1}). However, the tropical Pacific responses almost disappear, and the eastern Pacific anomalous Hadley cell is much weaker with no ascending branch south of the equator (Figs. 3b,c,f). This is mainly due to the absence of ocean upwelling/downwelling in the slab ocean, which amplifies the eastern tropical Pacific SST

anomalies in response to surface wind anomalies in the fully coupled model. The warming over the southern Indian Ocean in the slab ocean (Fig. 3b) excited by the tropical Atlantic heating disappears in the fully coupled model (Fig. 1c) because in the fully coupled model, the anomalous Indian Ocean gyre circulation leads to a divergence of oceanic heat transport there; thus, currents transport the heat supplied by the atmosphere away from there. With the slab ocean, such anomalous divergence of oceanic heat transport does not exist in the southern Indian Ocean, resulting in strong warming there (Fig. 3b). When we double the *q*-flux anomaly (the implied cross-equatorial ocean heat transport is reduced by 0.56 PW), the global integrated Hadley circulation anomaly reaches 90×10^9 kg s^{-1} (indicating a nonlinear response). The stronger reduction of precipitation over the central American region induces a significant southward shift of the ITCZ over the Pacific and associated warming south of the equator and cooling north of the equator in the eastern tropical Pacific. These changes have similar amplitudes to those in the fully coupled model. However, the southward shift of the ITCZ over the Pacific is almost zonally symmetric; thus, changes of the Walker circulation over the tropical Pacific are very weak without ocean dynamics.

4. Remote impacts on Indian and eastern Asian monsoons

In experiments with the fully coupled model, the weakening and eastward shifts of the Walker circulation over the southern tropical Pacific (Fig. 2a) reduce the summer precipitation over Indonesia by a maximum of 1.4 m yr^{-1} (Fig. 2f). The Rossby wave response to suppressed convective heating over Indonesia would weaken the Indian summer monsoon (Lau and Nath 2000). Indeed the modeled summer precipitation over the Indian southwest coast decreases by 0.84 from 2.2 m yr^{-1} in the control run. The southerly monsoon winds over the western Arabian Sea are weakened by 1.5 from 8.4 m s^{-1} in the control run, resulting in anomalous northerly surface winds there (Fig. 2f), consistent with the weakening of the southerly Indian summer monsoon winds and coastal upwelling during the Greenland stadials as indicated by paleorecords off the western boundary of the Arabian Sea (Altabet et al. 2002). For both experiments with a slab ocean, there is also a reduction of summer precipitation over the Indian southwest coast (about 1.5 m yr^{-1} in the experiment with doubled q-flux anomaly). The mechanism of this reduction, and its relationship to the anomalous warming over the southern Indian Ocean, has not been determined.

In experiments with the fully coupled model, the enhancement of the Walker circulation in the northern tropical Pacific (Fig. 2a) enhances summer precipitation north of the WPWP (Fig. 2f) and surface convergence at 22°N, 136°E (Fig. 2f), which weakens the eastern Asian summer monsoon and reduces summer precipitation over eastern China and the WPWP. Paleorecords from Hulu Cave (32°N, 119°E) in eastern China indicate that the ratio of summer to winter precipitation was significantly reduced during Greenland stadials (Wang et al. 2001), and in our fully coupled model, the ratio there is reduced from 3 in the control run to 2 in the perturbed run with the summer precipitation reduced by 0.6 (Fig. 2f) from 2 m yr^{-1} in the control run. For both experiments with a slab ocean, there is no statistically significant change of summer precipitation over eastern China because changes of the Walker circulation over the tropical Pacific are very weak. Paleoproxies also indicate a reduction of precipitation around the WPWP (6°N, 125°E, Stott et al. 2002; 8.8°N, 121°E, Dannenmann et al. 2003) during Greenland stadials. In the fully coupled model, the summer precipitation reduction at these two locations is 0.45 (out of 3.9 m yr^{-1} in the control run) and 0.76 m yr^{-1} (out of 4.1 m yr^{-1} in the control run), respectively (Fig. 2f). Similarly, there is no statistically significant change of summer precipitation at these locations for both experiments with a slab ocean.

5. Conclusions and discussion

Our idealized experiments show that a substantially weakened THC leads to significant and persistent remote responses outside the Atlantic. These include a southward shift of the ITCZ in the tropical Pacific, an El Niño–like condition and a weakened Walker circulation in the southern tropical Pacific, a La Niña–like condition and a stronger Walker circulation in the northern tropical Pacific, more symmetric western tropical Pacific Ocean circulation and global zonally averaged ITCZ position about the equator, and weakened Indian and east Asian summer monsoons. These changes are consistent with the global synchronization of abrupt climate changes as indicated by paleorecords, especially the antiphase precipitation change at Hulu Cave in China and northeastern Brazil. Our modeled tropical Pacific anomalies are asymmetric about the equator and are thus unlike those induced by transient El Niño events. We repeated the water hosing experiments with another GFDL fully coupled model (CM2.1; D05), and the tropical Pacific responses are very similar and robust. When coupled with a slab ocean with no ocean dynamics, we found that specify-

ing a stronger reduction of cross-equatorial Atlantic Ocean northward heat transport leads to a stronger cross-equatorial anomalous Hadley circulation; the tropical Pacific responses are much smaller given the same anomalous cross-equatorial ocean heat transport as in the fully coupled model. Even with doubled q-flux anomaly, the changes of Walker circulation over the tropical Pacific are still very weak, and there is no statistically significant change of the summer monsoon over eastern China. Ocean dynamics is very important for amplifying the tropical Pacific responses.

Our model results are derived using modern boundary conditions and then compared to proxy records from a glacial world. A recent study (Chiang et al. 2003) shows that the Atlantic ITCZ shifts southward in a coupled atmospheric general circulation and slab ocean model in response to the Last Glacial Maximum boundary conditions (primarily the land ice sheet). Future studies are necessary to assess how the simulated responses in our fully coupled model may differ under glacial boundary conditions. Nevertheless, the millennial-scale abrupt climate changes such as the Heinrich events and D–O cycles we compare with are not associated with large amounts of abrupt change in sea level height and volume of land ice sheets, and thus the mechanism modeled here would still be important. The weak tropical Pacific responses in many previous simulations might be due to the use of coarser resolution models, or to the use of less intense freshwater forcing. Our modeled tropical Pacific SST anomaly could still be underestimated and might be increased with even higher resolution models.

Acknowledgments. We thank Isaac Held, Gabriel Lau, and Kirk Bryan for very helpful discussions; Thomas Knutson for the help with the slab ocean model; and many GFDL colleagues for the development of the coupled model used in this study. We thank Michael Winton, Anthony Rosati, and Ronald Stouffer for the internal review of the paper. We thank the anonymous reviewers for valuable comments. The numerical experiments were carried with the supercomputer facilities at GFDL.

REFERENCES

Altabet, M. A., M. J. Higginson, and D. W. Murray, 2002: The effect of millennial-scale changes in Arabian Sea denitrification on atmospheric CO_2. *Nature,* **415,** 159–162.

Benway, H. M., A. C. Mix, B. A. Haley, and G. P. Klinkhammer, 2004: Eastern tropical Pacific paleosalinity and global climate change. *Eos, Trans. Amer. Geophys. Union,* **85** (Fall Meeting Suppl.) Abstract PP51C-1344.

Chiang, J. C. H., M. Biasutti, and D. S. Battisti, 2003: Sensitivity of the Atlantic ITCZ to Last Glacial Maximum boundary conditions. *Paleoceanography,* **18,** 1094, doi:10.1029/2003PA000916.

Clark, P. U., N. G. Pisias, T. F. Stocker, and A. J. Weaver, 2002: The role of the thermohaline circulation in abrupt climate change. *Nature,* **415,** 863–869.

Clement, A. C., M. A. Cane, and R. Seager, 2001: An orbitally driven tropical source for abrupt climate change. *J. Climate,* **14,** 2369–2375.

Dahl, K. A., A. J. Broccoli, and R. Stouffer, 2005: Assessing the role of North Atlantic freshwater forcing in millennial scale climate variability: A tropical Atlantic perspective. *Climate Dyn.,* **24,** 325–346.

Dannenmann, S., B. K. Linsley, D. W. Oppo, Y. Rosenthal, and L. Beaufort, 2003: East Asian Monsoon forcing of suborbital variability in the Sulu Sea during Marine Isotope Stage 3: Link to Northern Hemisphere climate. *Geochem. Geophys. Geosyst.,* **4,** 1001, doi:10.1029/2002GC000390.

Dong B. W. and R. T. Sutton, 2002: Adjustment of the coupled ocean–atmosphere system to a sudden change in the Thermohaline Circulation. *Geophys. Res. Lett.,* **29,** 1728, doi:10.1029/2002GL015229.

Koutavas, A., J. Lynch-Stieglitz, T. M. Marchitto Jr., and J. P. Sachs, 2002: El Niño–like pattern in Ice Age tropical Pacific sea surface temperature. *Science,* **297,** 226–230.

Latif, M., 2001: Tropical Pacific/Atlantic Ocean interactions at multi-decadal time scales. *Geophys. Res. Lett.,* **28,** 539–542.

Lau, N. C., and M. J. Nath, 2000: Impact of ENSO on the variability of the Asian–Australian monsoons as simulated in GCM experiments. *J. Climate,* **13,** 4287–4309.

Lea, D. W., D. K. Pak, and H. J. Spero, 2000: Climate impact of late Quaternary equatorial Pacific sea surface temperature variations. *Science,* **289,** 1719–1724.

McManus, J. F., R. Francois, J. M. Gherardi, L. D. Keigwin, and S. Brown-Leger, 2004: Collapse and rapid resumption of Atlantic meridional circulation linked to deglacial climate changes. *Nature,* **428,** 834–837.

Peterson, L. C., G. H. Haug, K. A. Hughen, and U. Rohl, 2000: Rapid changes in the hydrologic cycle of the tropical Atlantic during the last glacial. *Science,* **290,** 1947–1950.

Saenko, O. A., A. Schmittner, and A. J. Weaver, 2004: The Atlantic–Pacific seesaw. *J. Climate,* **17,** 2033–2038.

Stott, L., C. Poulsen, S. Lund, and R. Thunell, 2002: Super ENSO and global climate oscillations at millennial time scales. *Science,* **297,** 222–226.

Vellinga, M., and R. A. Wood, 2002: Global climate impacts of a collapse of the Atlantic thermohaline circulation. *Climate Change,* **54,** 251–267.

Wang, X. F., A. S. Auler, R. L. Edwards, H. Cheng, P. S. Cristalll, P. L. Smart, D. A. Richards, and C. C. Shen, 2004: Wet periods in northeastern Brazil over the past 210 kyr linked to distant climate anomalies. *Nature,* **432,** 740–743.

Wang, Y. J., H. Cheng, R. L. Edwards, Z. S. An, J. Y. Wu, C.-C. Shen, and J. A. Dorale, 2001: A high-resolution absolute-dated late Pleistocene monsoon record from Hulu Cave, China. *Science,* **294,** 2345–2348.